Power Management Strategies for a Microgrid With Multiple Distributed Generation Units

F. Katiraei, *Member, IEEE*, and M. R. Iravani, *Fellow, IEEE*

***Abstract*—This paper addresses real and reactive power management strategies of electronically interfaced distributed generation (DG) units in the context of a multiple-DG microgrid system. The emphasis is primarily on electronically interfaced DG (EI-DG) units. DG controls and power management strategies are based on locally measured signals without communications. Based on the reactive power controls adopted, three power management strategies are identified and investigated. These strategies are based on 1) voltage-droop characteristic, 2) voltage regulation, and 3) load reactive power compensation. The real power of each DG unit is controlled based on a frequency-droop characteristic and a complimentary frequency restoration strategy. A systematic approach to develop a small-signal dynamic model of a multiple-DG microgrid, including real and reactive power management strategies, is also presented. The microgrid eigen structure, based on the developed model, is used to 1) investigate the microgrid dynamic behavior, 2) select control parameters of DG units, and 3) incorporate power management strategies in the DG controllers. The model is also used to investigate sensitivity of the design to changes of parameters and operating point and to optimize performance of the microgrid system. The results are used to discuss applications of the proposed power management strategies under various microgrid operating conditions.**

***Index Terms*—Distributed generation (DG), droop characteristics, eigen analysis, microgrid, power management, real and reactive power control, small-signal dynamic analysis.**

I. Introduction

PROLIFERATION of distributed resource (DR) units in the form of distributed generation (DG), distributed storage (DS), or a hybrid of DG and DS units has brought about the concept of microgrid [1]–[3]. A microgrid is defined as a cluster of DR units and loads, serviced by a distribution system, and can operate in 1) the grid-connected mode, 2) the islanded (autonomous) mode, and 3) ride-through between the two modes. The idea supporting the formation of the microgrid is that a paradigm consisting of multiple generators and aggregated loads is adequately reliable and economically viable as an operational electric system.

A power management strategy (PMS) is required for sound operation of a microgrid with multiple (more than two) DG units, particularly during the autonomous mode of operation. Fast response of PMS is more critical for a microgrid as compared with a large interconnected grid. The reasons are 1) presence of multiple small-DG units with significantly different power capacities and generation characteristics, 2) presence of no dominant source of energy generation during autonomous mode of operation, and 3) fast response of electronically interfaced DG (EI-DG) units, which can adversely affect voltage/angle stability if appropriate provisions are not in place.

The microgrid PMS assigns real and reactive power references for the DG units to 1) efficiently share real-/reactive-power requirements of loads among the DG units, 2) quickly respond to disturbances and transients due to the changes in the system operating mode, 3) determine the final power generation set-points of the DG units to balance power and restore frequency of the system, and 4) provide a means for re-synchronization of the autonomous microgrid with the main grid for reconnection. PMSs for a microgrid system and their impacts on the controls of DG units have neither been fully understood nor comprehensively investigated in the technical literature. The main objective of this paper is to cover this gap.

To investigate various PMSs, a three-DG microgrid study system is introduced. The system includes two EI-DG units and one conventional synchronous machine-based DG unit. The system represents all characteristics of a radial microgrid in terms of PMS requirements and their impacts on the microgrid behavior.

This paper also presents a methodology to systematically develop a small-signal dynamic model of a microgrid for eigen studies. Frequency variations of autonomous microgrid are also considered in the model. The model is general and can accommodate any microgrid configuration and any number of DG units. The model is used to 1) investigate the dynamic behavior, 2) select control parameters of DG units, and 3) imbed various PMSs in the DG controllers and investigate their impacts on the behavior of the study microgrid.

The rest of this paper is arranged as follows. Section II briefly describes the microgrid study system. Sections III and IV discuss the needs for PMSs and outline three PMSs adopted for the study microgrid. Sections V and VI deal with small-signal modeling and analysis of the microgrid system. Sections VII and VIII summarize the proposed PMSs and conclude the results obtained from eigen analysis of the study system.

II. Microgrid System

Fig. 1 shows a single-line diagram of a 13.8-kV distribution system used to investigate possible microgrid PMSs. The microgrid system includes a conventional DG unit, i.e., $DG1$ (1.8-MVA), connected to feeder 1, two EI-DG units, i.e., $DG2$ (2.5-MVA) and $DG3$ (1.5-MVA), connected to feeders 3 and 4

Manuscript received September 27, 2005; revised March 16, 2006. Paper no. TPWRS-00620-2005.

F. Katiraei is with the Natural Resource Canada at the CETC-Varrenes, Varennes, QC J3X 1S6, Canada (e-mail: farid.katiraei@nrcan.gc.ca).

M. R. Iravani is with the Department of Electrical and Computer Engineering, University of Toronto, Toronto, ON M5S 3G4, Canada (e-mail: iravani@ecf.utoronto.ca).

Digital Object Identifier 10.1109/TPWRS.2006.879260

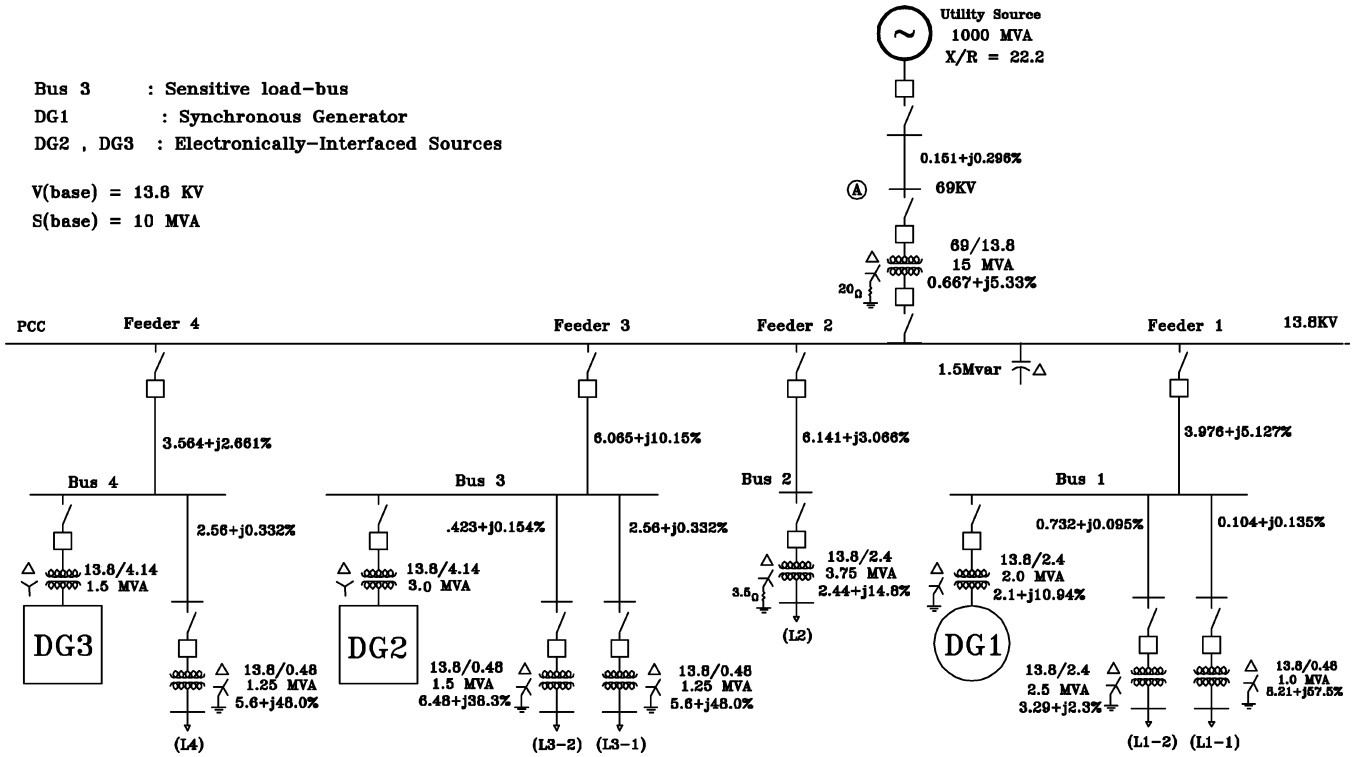

Fig. 1. Single-line diagram of the microgrid study system.

respectively. $DG1$ represents a slow-response DG unit, e.g., a diesel-generator or a gas-fired unit equipped with excitation and governor control systems. $DG2$ and $DG3$ are fast-acting, dispatchable sources. It is assumed that $DG2$ and $DG3$ each has adequate capacity to supply independently controlled real and reactive power to the system, within limits, based on pre-specified control commands. It should be noted that the PMSs discussed in this paper are only applicable to dispatchable DG units. Non-dispatchable sources are controlled based on optimal power generation schemes to deliver maximum available power [4].

The three-DG system can be used to investigate possible interaction phenomena 1) among EI-DG units, 2) between EI-DG units and conventional DG units, and 3) between DG units and the network. The focus of this paper is on the interaction phenomena and small-signal dynamics of DG units that are interfaced to the host utility grid through voltage-sourced converters (VSCs). The dynamic behavior of the conventional DG unit is relatively well known [5] and is not emphasized in this paper.

III. Power Management Strategy of a Microgrid

Regardless of the microgrid mode of operation, i.e., 1) grid-connected, 2) islanded (autonomous), or 3) transition between the two modes, the adopted PMS has a direct impact on the system operational behavior in terms of voltage/angle stability, power quality, and availability of service to consumers. In contrast to the philosophy of operation of interconnected power systems, in a microgrid system, none of the DG units acts as a spinning reserve or as a backup generation.

In the grid-connected mode, DG units are expected to supply pre-specified power, e.g., to minimize power import from the grid (peak shaving). Such requirements are system dependent and vary from system to system. In a grid-connected mode, similar to a conventional utility system, each DG unit can be controlled to generate pre-specified real and reactive power components (PQ-bus) or generate pre-specified real power and regulate its terminal voltage (PV-bus). The utility grid is expected to support the difference in real/reactive power requirements and maintain the frequency [6].

In the autonomous mode of operation, the available power of the DG units must meet the total load demand of the microgrid; otherwise, the system must undergo load shedding to match generation and load demand. In addition, fast and flexible real/reactive power control strategies are required to minimize the microgrid dynamics, e.g., due to islanding, and damp out system oscillations. This paper only considers PMSs based on locally measured signals when no communication exists among DG units. Thus, controllers should operate based on local information.

The main criteria that should be met by the PMS are as follows:

- load sharing among DG units while minimizing the total power loss of the system;
- consideration of specific limits of each DG unit, including type of the DG unit, cost of generation, time-dependency of the prime source, maintenance interval, and environmental impacts;
- maintaining the power quality inclusive of voltage profile, voltage fluctuations, and harmonic distortion;
- improving the dynamic response, maintaining stability margin, and voltage/frequency restoration of the system during and after transients.

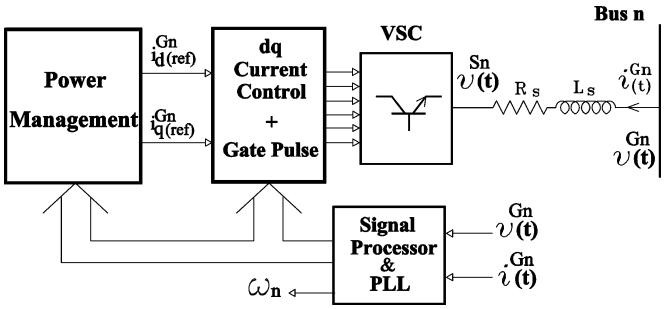

Fig. 2. Block diagram of nth EI-DG unit.

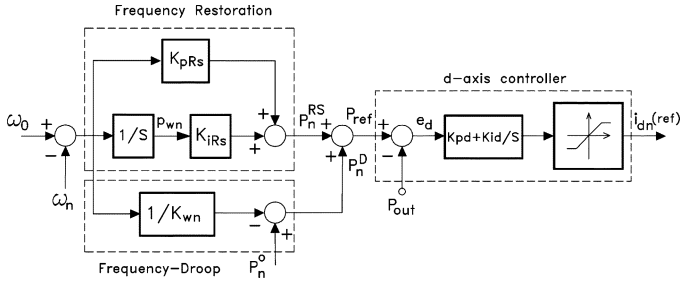

Fig. 3. Proposed real power controller for the nth EI-DG unit.

In the proposed microgrid system of Fig. 1, $DG1$ is equipped with governor and excitation systems with relatively slow responses for real and reactive power control. Thus, $DG1$ cannot rapidly contribute to the power management of the system during transient and small-signal dynamics. However, it participates in the slow dynamics and steady-state power management.

IV. PMS of an Electronically Interfaced DG Unit

Fig. 2 shows a block representation of the control system, the power management system, and the interface medium (VSC) of an EI-DG unit. The system utilizes independent real/reactive power control strategies to determine the output power requirements of the unit [7]. Controls are implemented in a $dq0$ reference frame that determines d- and q-axis components of the ac-side currents as described in [8]. The current set-points are determined by the power management block. The set-point of the d-axis current component determines real power generation of the unit. Similarly the set-point of the q-axis current component determines the reactive power injection/absorbtion of the unit.

A signal processing block and a phase-locked loop (PLL) circuit are used as the complimentary parts of the control systems (see Fig. 2) to process the measured currents and voltages of the DG unit and to estimate the local frequency at the DG-bus. The frequency estimation is used for synchronization and to independently track relative angle of the DG reference frame during transients [7]. This paper focuses on defining the real and reactive power control strategies and calculation of the d- and q-axis current references.

The power management system encompasses two parts: 1) the real power generation block that determines the real power output of the unit based on frequency variations at the point of common coupling (PCC) of the DG unit and 2) the reactive power control block that regulates voltage of the corresponding DG-bus or compensates reactive power of the load connected at the terminal. The two main building blocks of the power management system are explained in the following two subsections.

A. Real Power Management

Real power generation of an EI-DG unit is specified based on a frequency-droop characteristic [9] and a frequency restoration algorithm [10]. This method is chosen since the frequency of the microgrid, during an autonomous mode of operation, freely varies when none of the DG units can dominantly enforce the base frequency of the system. The frequency deviations can be limited by introducing the frequency-droop characteristic that uses the microgrid frequency as a communication means, among the fast acting EI-DG units, to dynamically balance the real power generation of the islanded microgrid. During the grid-connected mode, where the frequency of the system is fixed, real power generation of the DG units is controlled by the real power references assigned to the units.

Fig. 3 shows a generic real power management block for the EI-DG units of a microgrid. Input to the block is the local frequency (ω_n), estimated by a conventional PLL using bus voltages [11] (see Fig. 2). Output of the block is the reference current for the d-axis inner current controller of the unit, corresponding to the real power reference of the unit (P_{ref}). The real power reference is

$$P_{ref} = P_n^D + P_n^{RS} \tag{1}$$

where P_n^D corresponds to variations in the local frequency, determined from the frequency-droop characteristic, to supply adequate power to the load or damp power oscillations, and P_n^{RS} is to restore the steady-state frequency of the system.

Typical frequency-droop characteristics are shown in Fig. 4 in which the $\omega - P$ characteristics for the nth and the mth EI-DG units are presented. A $\omega - P$ characteristic can be mathematically represented as

$$P_n^D = -\frac{1}{K_{wn}}(\omega_o - \omega_n) + P_n^o \tag{2}$$

where K_{wn} is the characteristic slope for the nth DG unit, ω_o is the reference frequency of the microgrid, and P_n^o represents the initial power generation assigned to the unit. In the case of multiple-DG units with different capacities serving a microgrid, slopes of $\omega - P$ characteristics should satisfy

$$S_{G_n} K_{wn} = S_{G_m} K_{wm},\ \forall n, m \tag{3}$$

where S_{G_n} and S_{G_m} are the rated power capacities of the nth and the mth units, respectively. Equation (3) indicates that the load demand is shared among the DG units proportional to the capacities of units.

To restore the frequency of the islanded microgrid, a frequency restoration algorithm, as shown in Fig. 3, is needed. The frequency restoration term is extracted from deviations in the

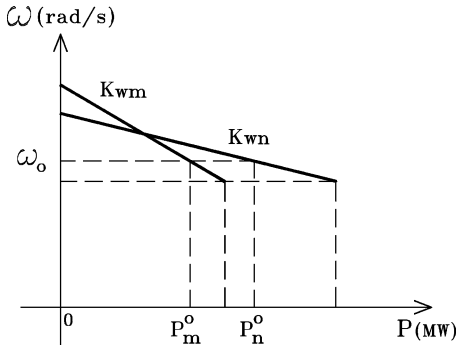

Fig. 4. Frequency-droop characteristics for the nth and the mth EI-DG units.

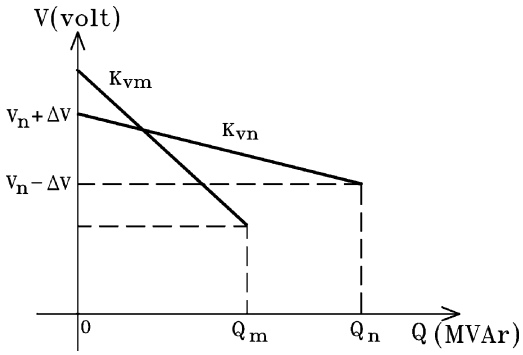

Fig. 6. Voltage-droop characteristics for the nth and the mth EI-DG units.

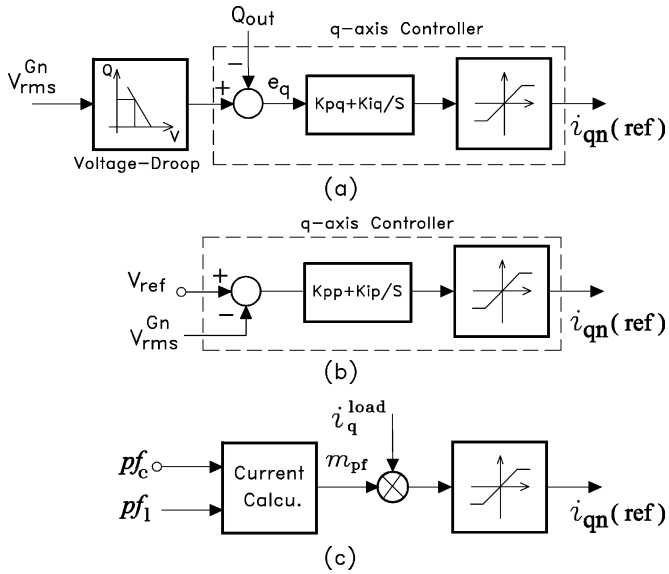

Fig. 5. Reactive power control strategies for an EI-DG unit. (a) Voltage-droop characteristic method. (b) Voltage regulation method. (c) Reactive power compensation method.

local frequency of the system, using a PI controller with a large time constant. The frequency restoration term is

$$P_n^{RS} = \left(K_{pRs} + \frac{K_{iRs}}{s}\right)(\omega_o - \omega_n) \tag{4}$$

where K_{pRs} and K_{iRs} represent the proportional and the integral gains of the controller. A state-space model of the real power controller is derived in Appendix A.

B. Reactive Power Management

Three strategies are defined in which the reactive power of a EI-DG unit is controlled to 1) prevent deviations in terminal voltages using a pre-set V-Q characteristic [12], 2) achieve voltage regulation at a specific load-bus [13], or 3) compensate reactive power demand of a load based on the power factor set-point of the load [13]. These reactive power strategies are explained in the following sections.

1) Strategy I: Voltage-Droop Characteristic: Fig. 5(a) shows a reactive power control strategy based on a voltage-droop characteristic, including a V-Q characteristic to determine reactive power reference Q_{ref} of the unit and a PI controller to assign the q-axis current $i_{qn}(ref)$. Input to the block is the rms value of the voltage at PCC of the DG unit. A pre-set V-Q characteristic is used to determine the reference for reactive power of the unit.

The PI controller specifies the corresponding q-axis current set-point to adjust the reactive power generation of the unit, Q_{out}, to the reference value. Thus, reactive power of the EI-DG unit varies based on deviations in the bus voltage. Therefore, the EI-DG unit responds to voltage deviations caused either by the system or the local load. Typical voltage-droop characteristics are shown in Fig. 6. The slope of the V-Q characteristic is calculated based on the permitted range of variations for the terminal voltage of each EI-DG unit and in compliance with the multiple DG slope relationship given by

$$S_{G_n} K_{vn} = S_{G_m} K_{vm},\ \forall n, m \tag{5}$$

where K_{vn} and K_{vm} are slopes of the V-Q characteristics for the nth and the mth units, respectively. Condition (5) implies that the slope of the V-Q characteristic for the nth DG unit is calculated proportional to its rated power capacity, S_{Gn}. A state-space model of the reactive power controller, based on the voltage-droop characteristic, is developed in Appendix A.

2) Strategy II: Voltage Regulation: Reactive power control strategy based on voltage regulation is described in Fig. 5(b). Reactive power of the EI-DG unit is controlled to regulate the PCC voltage at a pre-specified level (normally 1 p.u.). Thus, this control strategy can be interpreted as a special case of voltage-droop characteristic, where the tangent of the V-Q characteristic is set to zero and implicitly specifies reactive power reference of the unit. In Fig. 5(b), $i_{qn}(ref)$ is generated from deviations in the rms value of the terminal voltage with respect to the preset reference voltage, through a PI controller. The reactive power strategy is only applied to those buses in a microgrid system that supply sensitive loads with very limited tolerance for voltage variations. The approach presented in Appendix A can be used to derive a state-space model of the reactive power controller based on the voltage-regulation strategy.

3) Strategy III: Power Factor Correction: This strategy is normally utilized to improve power factor or to meet reactive power requirements of a load through a fast reactive power variation characteristic [13]. This control strategy is adopted for the microgrid system to locally compensate reactive power of

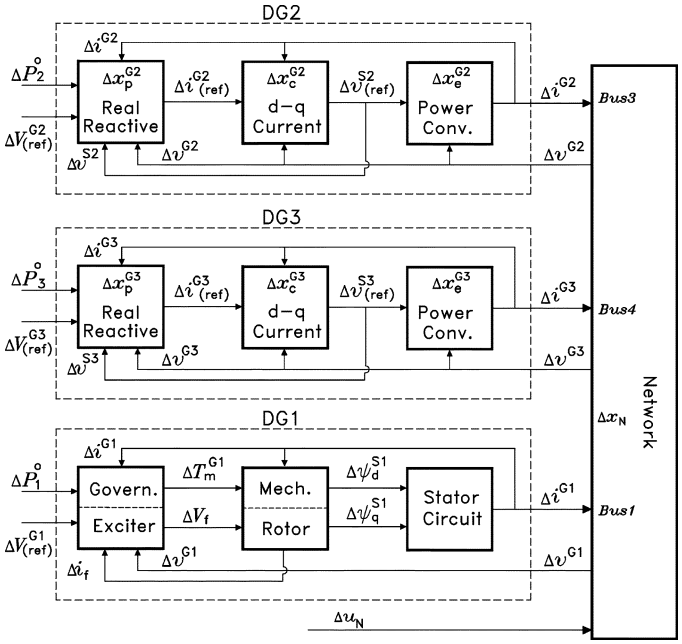

Fig. 7. Small-signal model of microgrid system of Fig. 1.

a load by a DG unit connected to the load-bus. Thus, the load power factor is assigned at a pre-set value regardless of the load variations. The reactive power compensation block is shown in Fig. 5(c). The reference value for the q-axis component of the DG current, $i_{qn}(ref)$, is given by

$$i_{qn}(ref) = m_{pf} i_q^{\text{load}} \tag{6}$$

where i_q^{load} is the q-component of the load current, and m_{pf} is the compensation factor. The compensation factor m_{pf}, the load power factor pf_L, and the desired power factor pf_C are related by

$$pf_C = \frac{pf_L}{\sqrt{pf_L^2 + (1 - m_{pf})(1 - pf_L^2)}}. \tag{7}$$

In (7), $m_{pf} = 0$ stands for no compensation ($pf_C = pf_L$), and $m_{pf} = 1$ means full compensation of the load reactive power ($pf_C = 1.0$). The approach of Appendix A can be used to derive the state-space model of the reactive power controller based on power factor correction.

V. Small-Signal Dynamic Model of Microgrid

A linearized mathematical model of the microgrid system (see Fig. 1) in the standard form of

$$\Delta \dot{x} = A\Delta x + B\Delta u \tag{8}$$

is developed to 1) design the controllers, 2) investigate applicability of the PMSs, 3) examine system sensitivity to parameter variations, and 4) analyze system dynamics subsequent to internal and external disturbances [14]. The developed small-signal dynamic model also takes into account frequency deviations of the microgrid during an autonomous mode. Fig. 7 shows a block representation of the small-signal dynamic model of the microgrid system of Fig. 1 during an autonomous mode of operation. The system is comprised of four subsystems, namely, 1) $DG1$ and its excitation and governor systems connected at Bus-1, 2) $DG2$ and its real/reactive power management controllers connected at Bus-3, 3) $DG3$ and its corresponding real/reactive power management controllers connected at Bus-4, and 4) the network including the distribution lines, the loads, and the fixed capacitor bank connected to the microgrid PCC.

TABLE I
Operating Point for the Microgrid System of Fig. 7

	Generation	Consumption
DG1	1.46 MW / 0.59 MVAr	--------
DG2	1.87 MW / 1.06 MVAr	--------
DG3	0.96 MW / 0.41 MVAr	--------
Load 1	--------	1.21 MW / 0.81 MVAr
Load 2	--------	0.6 MW / 0.42 MVAr
Load 3	--------	1.5 MW / 0.95 MVAr
Load 4	--------	0.9 MW / 0.61 MVAr
Capacitor Cp	1.0 MVAr	--------

The lines and the constant loads are represented by series-connected RL branches in each phase and, where applicable, lumped together and mathematically represented by the corresponding differential equations. The nonlinear and variable parts of the loads, e.g., at Bus-3 and Bus-4 in Fig. 1, are represented by equivalent current sources at the fundamental frequency and considered as inputs for the network subsystem.

To develop the linearized mathematical model of the overall system, first, the state-space representation of each subsystem is formed. Then, the state-space representations are transferred to a global reference frame and combined based on input/output relationships shown in Fig. 7 [8]. The modeling approach is general and can be extended to represent a microgrid with an arbitrary number of conventional DG and EI-DG units. A systematic approach to develop a small-signal dynamic model of each subsystem in Fig. 7 and to construct the overall model (8) are detailed in [8]. Appendexes B and C briefly outline the small-signal dynamic models for an EI-DG and a conventional DG unit, respectively, to demonstrate the procedures to incorporate the PMSs in the microgrid models.

VI. Small-Signal Dynamics

The linearized model given by (8) is used to investigate the small-signal dynamics of the microgrid of Fig. 1 during an autonomous mode of operation. The initial steady-state operating point of the microgrid is given in Table I. In this operating point, $DG1$, $DG2$, and $DG3$ predominantly supply their local loads, i.e., Load-1, Load-3, and Load-4, respectively, and Load-2 is supplied by the excess power of the DG units.

A. System Oscillatory Modes

For the given operating point, the system is stable, and Table II shows the eigenvalues of the oscillatory modes of the system corresponding to two case studies.

- CASE I: Real and reactive power management strategies of $DG2$ and $DG3$ are based on frequency-droop and voltage-droop characteristics.

TABLE II
COMPLEX EIGENVALUES OF THE SYSTEM FOR CASES I AND II

Eigen values	Case I		Case II	
	Real (1/s)	Im. (rad/s)	Real (1/s)	Im. (rad/s)
1,2	- 219.556	± 2164.05	- 2298.7	± 2139.14
3,4	- 366.93	± 1175.57	- 290.0	± 1278.64
5,6	- 68.0	± 725.9	- 62.6	± 706.99
7,8	- 39.56	± 507.59	- 81.71	± 456.86
9,10	- 110.71	± 427.52	- 113.44	± 420.54
11,12	- 1710.09	± 389.43	- 1709.07	± 380.86
13,14	- 748.57	± 380.52	- 747.09	± 377.24
15,16	- 365.37	± 386.08	- 361.29	± 374.22
17,18	- 425.76	± 377.0	- 425.75	± 376.98
19,20	- 56.46	± 336.43	- 143.99	± 291.09
21,22	- 193.0	± 77.35	- 112.32	± 39.41
23,24	- 0.738	± 9.98	- 0.86	± 10.0

- CASE II: This case is similar to CASE I, except that reactive power management of $DG3$ is based on voltage-regulation characteristic.

Table II indicates that the microgrid system, under both PMSs, exhibits 12 pairs of complex conjugate eigenvalues. Eigenvalues 1 to 22 correspond to the electrical modes and controller modes and also represent interactions either among DG units or between DG units and the network. Eigenvalues 23 and 24 represent the mechanical oscillatory mode of $DG1$ with respect to the rest of the system.

Except the oscillatory mode corresponding to eigen pair (23,24), all the other system oscillatory modes identified in Table II have high natural frequencies and/or high dampings. Thus, they rapidly decay to zero subsequent to a disturbance, and their impacts on the system time response are not pronounced. The oscillatory mode represented by eigen pair (23,24), which corresponds to the mechanical oscillatory mode of DG1 with respect to the electrical system, has a low frequency and a relatively low damping. Thus, it has a dominant and detrimental impact on the system response after a disturbance. Therefore, after each disturbance, the mechanical oscillations of $DG1$ dominate the system dynamic behavior. These oscillations are experienced for several seconds and have detrimental effect on the microgrid behavior, e.g., power swings. The frequency of the inertial mode primarily depends on the initial loading of $DG1$ and approximately varies in the range of 0.1 to 3 Hz. Table II indicates that the damping and frequency of the mechanical oscillatory mode of $DG1$ are not significantly affected by the PMSs adopted for the microgrid.

Table III shows participation of each state variable of the system to the oscillatory modes for Case I. The participation factors are normalized such that the maximum value, in each row, is unity [15]. Participation factors with the value of less than 0.1 are not entered in Table III. The participation factors, for instance, illustrate that the state variables of control systems of all DG units have noticeable impact on the electromechanical mode represented by eigenvalues 23 and 24. Table III also shows that the state variables corresponding to the stator winding of $DG1$ and the network, lines 1 to 3, noticeably contribute in most of the system modes. This reveals the fact that ignoring dynamics of stator of $DG1$ and also distribution lines may lead to wrong results.

TABLE III
PARTICIPATION FACTORS OF THE SYSTEM STATES (CASE I)

	System states	Eigenvalues (Case I)											
		1,2	3,4	5,6	7,8	9,10	11,12	13,14	15,16	17,18	19,20	21,22	23,24
DG1	Stator	0.775	0.836	0.881	1.0	0.778	0.941	0.921	1.0	0.124	0.83	0.64	0.751
	Exciter				0.345	0.299		0.12	0.226		0.427	0.931	1.0
	Rotor												1.0
DG2	Converter		0.115	1.0	0.719	1.0			0.132		0.326		0.276
	Control		0.164	1.0	0.718	1.0			0.146		0.323	0.652	0.87
DG3	Converter		0.287	0.565	0.695	1.0		0.292	0.465		0.91	0.49	1.0
	Control		0.286	0.562	0.695	1.0		0.291	0.462		0.91	1.0	1.0
Lines	Line 1	0.94	0.961	0.93	0.995	0.712	1.0	0.587	0.762		0.787	0.559	0.8
	Line 2	0.131		0.14	0.324	0.814	0.104	0.189	0.556	1.0	0.27	0.124	0.2
	Line 3	0.138	0.191	0.423	0.5	0.285	0.135	0.278	0.299	1.0	0.75	0.43	0.8
PCC	Cap Bank	1.0	0.895	0.573	0.322		0.784	0.364	0.263		0.13	0.18	0.264
	Par. Load							1.0					

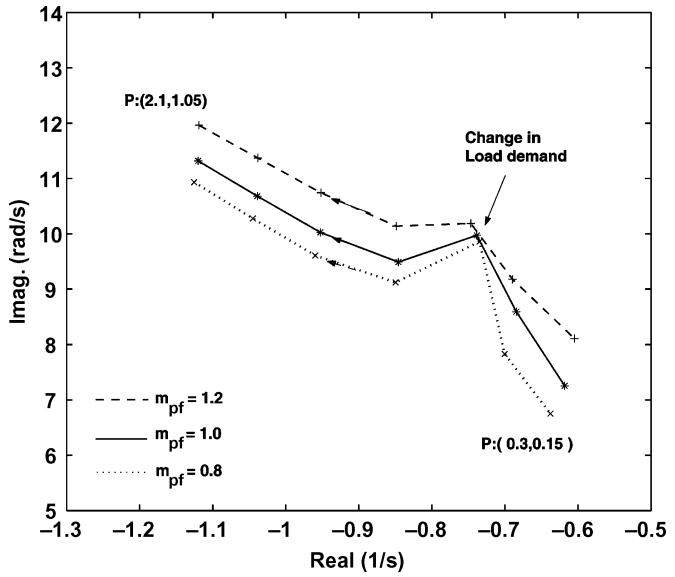

Fig. 8. Trace of the mechanical mode of the system for real power variations of DG2/DG3 between 0.3-MW/0.15-MW to 2.1-MW/1.05-MW (m_{pf}: reactive power compensation factor).

Using participation factors given in Table III, it can be concluded that eigen pairs (19,20) and (21,22) correspond to interactions among the DG units through their control systems. Table II shows that the damping and frequencies of these modes are highly dependent on the power management strategy. The frequency of these modes normally vary from a few Hertz, e.g., 5 Hz, up to about 55 Hz. Therefore, to accurately predict behavior of these modes, the electrical network must be represented as a dynamic system, i.e., by ordinary differential equations, and not as a static system based on algebraic phasor equations. Algebraic representation of the electrical network for such studies [12], [15] either eliminates such oscillatory modes or represents them by real eigenvalues, in spite of the fact that they exist as oscillatory modes and can even exhibit low dampings.

B. Sensitivity Analysis

A sensitivity analysis can reveal the dependency of the eigenvalues on the system and the controller parameters and to identify the acceptable ranges of variations in the control parameters.

1) Impact of DG Operating Point: Fig. 8 shows loci of the eigenvalues corresponding to the electromechanical mode of $DG1$ as the output real/reactive power of $DG2/DG3$ increases from 0.3-MW/0.15-MW to 2.1-MW/1.05-MW in

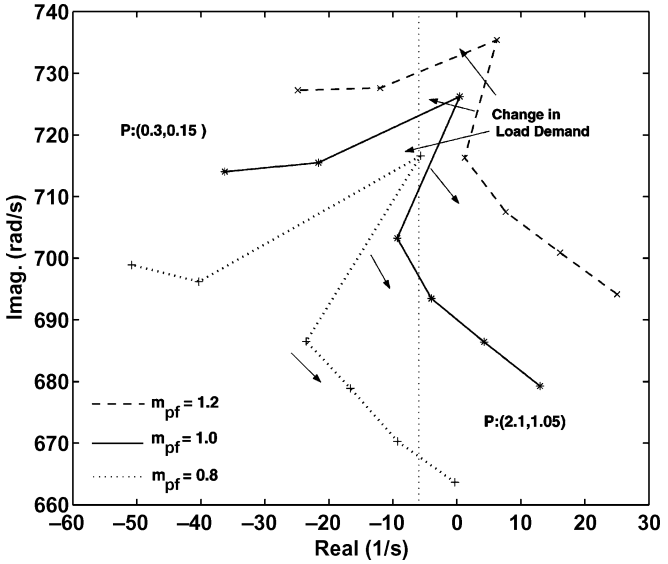

Fig. 9. Trace of the oscillatory mode corresponding to eigenvalues (5,6) for real power variations of DG2/DG3 between 0.3-MW/0.15-MW to 2.1-MW/1.05-MW (m_{pf}: reactive power compensation factor).

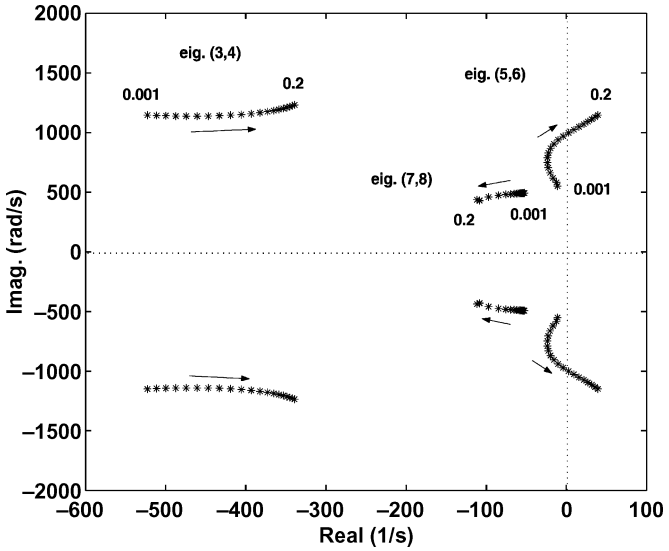

Fig. 10. Loci of eigenvalues (3,4), (5,6), and (7,8) (K_{pd2} of $DG2$ is changed from 0.001 to 0.2).

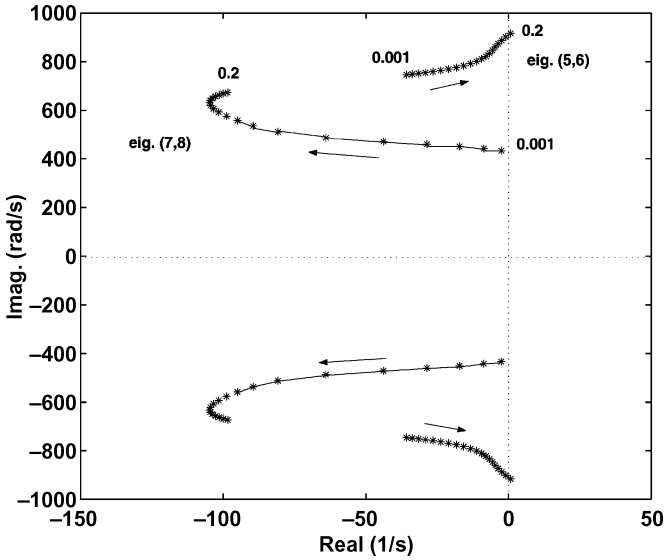

Fig. 11. Loci of eigenvalues (5,6) and (7,8) (K_{pd3} of $DG3$ is changed from 0.001 to 0.2).

steps of 0.3-MW/0.15-MW. The adopted PMSs for $DG2$ and $DG3$ are based on the frequency-droop and the voltage-droop characteristics. Fig. 8 shows the eigenvalue loci for three compensation levels of $m_{pf} = 0.8$, 1.0, and 1.2 corresponding to 80%, 100% and 120% compensation levels given by (7). Fig. 8 indicates that as power contributions of $DG2$ and $DG3$ increase, the damping and frequency of the electromechanical mode increases.

Increase in real power output of $DG2$ and $DG3$ (EI-DG units) primarily reduces real power supply of $DG1$ to maintain the balance between the power generation and consumption during the islanded mode of operation. In order to further increase real power of EI-DG units to demonstrate impact of change in operating point on oscillatory modes of the system, after specific point as shown in Fig. 8, the microgrid load needs to be increased to maintain power balance condition, while $DG1$ also contributes in real power generation of the microgrid.

Fig. 9 illustrates loci of the oscillatory mode corresponding to eigen pair (5,6) for the same real and reactive power variations described for Fig. 8. Eigen pair (5,6) represents one of the oscillatory interaction modes of the DG units and the rest of the microgrid, and its damping and frequency is highly dependent on the microgrid operating condition. Fig. 9 shows that the mode can become unstable by increasing real power outputs of $DG2$ and $DG3$. Fig. 9 also shows that the mode is marginally stable for the operating points with no significant power flow throughout the microgrid and high levels of reactive power compensation.

The directions of the eigenvalue migrations in Figs. 8 and 9 are opposite of each other, as real and reactive power outputs of $DG2$ and $DG3$ increase. This behavior demonstrates the essential role of the EI-DG units in stabilizing the system. However, the system stability is marginal under reactive power overcompensation ($m_{pf} \geq 1.0$ in Fig. 9). This indicates that reactive power management based on Strategy II (voltage regulation) or Strategy III (power factor correction) is the appropriate choice when DG units are assigned to locally compensate the reactive power requirements of the loads and dedicate most of their capacities to supply the real power demand of the microgrid.

2) Sensitivity to Control Parameters: Sensitivity of the system eigenvalues to variations in the proportional gains of the real power controllers K_{pd2}/K_{pd3}, and gains of the reactive power controllers K_{pq2}/K_{pq3}, of $DG2$ and $DG3$ are demonstrated in Figs. 10–13. Fig. 10 illustrates loci of three dominant pairs of microgrid eigenvalues for K_{pd2} variations in the range of 0.001 to 0.2. It shows that by increasing K_{pd2}, eigenvalues (5,6) depart to the right-hand plane (RHP), while eigenvalues (3,4) and (7,8) are displaced only within the left-hand plane (LHP). Similar results are observed for variations in K_{pd3} of $DG3$ controller in the range of 0.001 to 0.2, as shown in Fig. 11. However, K_{pd3} can be varied in a wider range in comparison to that of K_{pd2}. This shows that the stability of the microgrid is

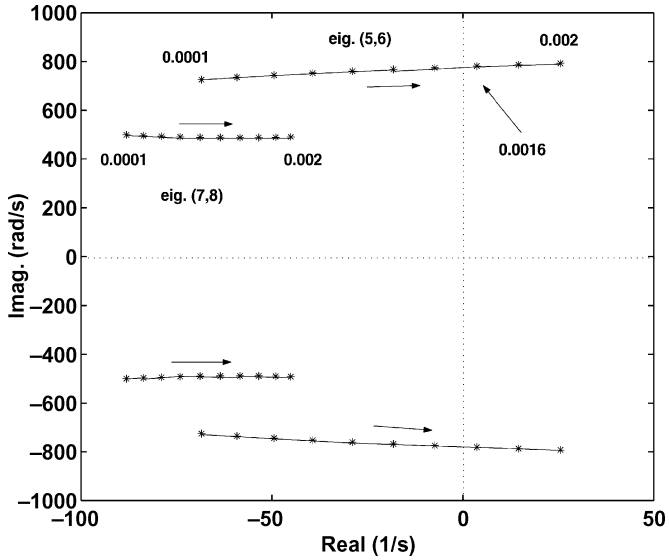

Fig. 12. Loci of two pairs of eigenvalues (5,6) and (7,8) (K_{pq2} of $DG2$ is changed from 0.0001 to 0.002).

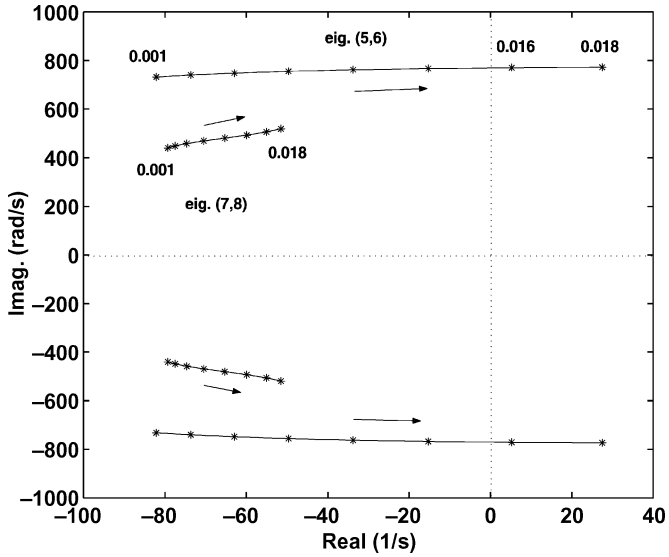

Fig. 13. Loci of two pairs of eigenvalues (5,6) and (7,8) (K_{pq3} of $DG3$ is changed from 0.0001 to 0.02).

less sensitive to the real power generated by the smaller unit, $DG3$, than that of $DG2$. The optimum values of the control parameters are chosen based on the locations of eigenvalues (3,4), (5,6), and (7,8).

Fig. 12 shows loci of eigenvalues (5,6) and (7,8) corresponding to variations of K_{pq2} of $DG2$ in the range of 0.0001 to 0.002. It illustrates that increasing K_{pq2} beyond 0.0016 leads to the departure of eigenvalues (5,6) to RHP. Similar to the results obtained for variations in K_{pd3} of Fig. 11, reactive power control gain K_{pq3} of $DG3$ can vary in a wider range, i.e., up to 0.014, without loss of stability (see Fig. 13). Based on the loci of eigenvalues (5,6) and (7,8), K_{pq2} and K_{pq3} must have relatively small values.

VII. Discussion

To evaluate performance of the microgrid under the adopted PMSs, the linearized model of the overall system, including the selected PMS, is developed and analyzed using an extended version of the eigenvalue method presented in [8]. The eigen analysis results are used to optimize the system performance under each PMS. The oscillatory modes of the system and participations of the state variables in the microgrid modes are compared for two cases. The studies show the following.

- The operating conditions at which real power is dominantly supplied by fast-acting $DG2$ and $DG3$ units provide high stability margins. In addition, reactive power outputs of DG units should be limited not to overcompensate the load. The reactive PMSs based on voltage-droop characteristic and voltage-regulation can cause overcompensation and require limits on reactive power controllers.
- Control parameters, including gains of real and reactive power controllers, effectively change damping ratio of the DG-network oscillatory modes of the microgrid. Appropriate selection of the control parameters based on eigenvalue results ensures the desired system performance and preserves adequate stability margin for the microgrid.
- Relative location and electrical proximity of DG units are important criteria for power management and generation planning of the microgrid. These affect the interaction modes of the DG units. For the DG units that are located in close electrical proximity to each other, independent reactive PMSs, i.e., voltage-regulation and reactive power compensation, are recommended.

VIII. Conclusions

This paper introduces three PMSs for an autonomous microgrid system. To investigate dynamic behavior of a microgrid under the proposed PMSs, a small-signal dynamic model for a multiple-DG microgrid system is developed. The model represents the dynamics of conventional and electronically interfaced DG units and the network and also accounts for the frequency deviation during microgrid autonomous operation. The model is adopted to examine the eigen-structure of a three-DG microgrid and to systematically 1) evaluate the microgrid stability, 2) design and optimize control parameters, 3) investigate the impact of PMS on the microgrid dynamics, especially after islanding incidents, and 4) evaluate interactions between DG unit and the network. The studies indicate that controls of electronically interfaced DG units and the adopted PMS have significant impact on the microgrid dynamic behavior when islanded from the grid and operates as an autonomous island.

Appendix A
Linearized Model of Real/Reactive Power Controllers

The linearized model of real power controller of an EI-DG unit, based on the frequency-droop characteristic and the frequency restoration algorithm shown in Fig. 2, is derived from (2) and (4), and the ODEs representing d-axis reference controller are

$$\begin{aligned} \Delta \dot{i}_{idn} &= \Delta P_{ref} - \Delta P_{out} \\ \Delta i_{dn}(ref) &= K_{id}\Delta i_{idn} + K_{pd}(\Delta P_{ref} - \Delta P_{out}) \end{aligned} \quad (9)$$

where Δi_{idn} is the state variable for the d-axis reference controller, and K_{pd} and K_{id} are the proportional and the integral gains of the controller, respectively. ΔP_{out} in (9) is represented by the linearized equation of the instantaneous real power in the $d-q$ frame

$$\Delta P_{out} = v_d^{oSn}\Delta i_d^{Gn} + v_q^{oSn}\Delta i_q^{Gn} + i_d^{oGn}\Delta v_d^{Sn} + i_q^{oGn}\Delta v_q^{Sn} \tag{10}$$

where Δi^{Gn} and Δv^{Gn} represent output currents and voltages of the EI-DG in the dq frame, and superscript "o" represents the steady-state operating value. The real power management block is fully described by the following state equations:

$$\begin{aligned}\Delta \dot{i}_{idn} = &\left(\frac{1}{K_{wn}} - K_{pRs}\right)\Delta\omega_n \\ &+ K_{iRs}\Delta p_{wn} - \left[v_{qn}^{osn} v_{dn}^{osn}\right]\Delta i^{Gn} \\ &- \left[i_{qn}^{oGn} i_{dn}^{oGn}\right]\Delta v^{sn} + \Delta P_n^o \end{aligned} \tag{11}$$

$$\Delta \dot{p}_{wn} = -\Delta\omega_n \tag{12}$$

$$\begin{aligned}\Delta \dot{\omega}_n = &-K_{pll}K_{pw}\Delta\omega_n \\ &- K_{pll}K_{iw}[m_q m_d]\Delta v^{Gn}\end{aligned} \tag{13}$$

where $\Delta\omega_n$ is the angular frequency of the dq reference frame for the nth DG unit, determined by a conventional PLL block [8]. The linearized model of the PLL is represented by (13), where K_{pll} is the amplifier gain corresponding to the amplitude of the input signal to the main PLL block, i.e., bus voltage Δv^{Gn}, and K_{pw} and K_{iw} are proportional and integral gains of the loop filter (LF). m_d and m_q are two constants relating d- and q-components of the bus voltage to the angle estimation block [8].

The linearized model of the reactive power controller is derived from the ODEs representing each reactive PMS of Fig. 5. Here, the modeling approach for the reactive PMS based on a voltage-droop characteristic of Fig. 5(a) is explained. The detailed model for the other two reactive PMSs are given in [14]. The reactive power controller based on voltage-droop is composed of 1) a V-Q characteristic determining the reference value for reactive power of the nth DG unit corresponding to the variations in its bus voltage and 2) a q-axis reference controller [see Fig. 5(a)]. The small-signal dynamic model of the reference controller is

$$\Delta \dot{q}_{iq} = \Delta Q_{ref} - \Delta Q_{out} \tag{14}$$

$$\Delta i_{qn}(ref) = K_{iq}\Delta q_{iq} + K_{pq}(\Delta Q_{ref} - \Delta Q_{out}) \tag{15}$$

where

$$\Delta Q_{ref} = \frac{1}{K_{vn}}\Delta v_{rms}^{Gn} + \Delta V^{Gn}(ref) \tag{16}$$

$$\begin{aligned}\Delta Q_{out} = &\, v_q^{oSn}\Delta i_d^{Gn} + i_d^{oGn}\Delta v_q^{Sn} \\ &- v_d^{oSn}\Delta i_q^{Gn} - i_q^{oGn}\Delta v_d^{Sn}\end{aligned} \tag{17}$$

and Δq_{iq} is the state variable of the PI controller of the reactive power control loop in Fig. 5(a). Thus, substituting for ΔQ_{ref} and ΔQ_{out} from (16) and (17) in (14) forms the state equation for the reactive power controller

$$\begin{aligned}\Delta \dot{q}_{iq} = &\frac{1}{K_{vn}v_{rms}^{oGn}}\left[v_q^{Gn} v_d^{Gn}\right]\Delta v^{Gn} - \left[-v_d^{oSn} v_q^{oSn}\right]\Delta i^{Gn} \\ &- \left[i_d^{oGn} i_q^{oGn}\right]\Delta v^{Sn} + \Delta V^{Gn}(ref).\end{aligned} \tag{18}$$

APPENDIX B
SMALL-SIGNAL DYNAMIC MODEL OF AN EI-DG UNIT

An EI-DG unit is composed of three main blocks: 1) the power management block, 2) the converter controls, and 3) the converter power circuit.

A. Power Management Block

The linearized dynamic model of a power management block for an EI-DG unit is shown in Fig. 7, for $\mathrm{n} = 2$ and 3. A systematic approach to form state equations of the power management block is explained in Appendix A. Using (11)–(13) and (18), the state-space representation of the power management block is derived as

$$\begin{aligned}\Delta \dot{x}_p^{Gn} = &A_p\Delta x_p^{Gn} + E_i^p\Delta i^{Gn} + E_{Gn}^p\Delta v^{Gn} \\ &+ E_{Sn}^p\Delta v^{Sn} + B_{Gn}^u\Delta u_{Gn}\end{aligned} \tag{19}$$

where Δx_p^{Gn} is the vector of state variables, Δi^{Gn} is the vector of converter output currents, Δv^{Gn} is the vector of corresponding bus voltages, Δv^{Sn} is the vector of converter output voltages, and Δu_{Gn} is the vector of input signals. The output from this block is the vector of reference currents $\Delta i^{Gn}(ref)$ for the d- and q-axis current controllers given by

$$\begin{aligned}\Delta i^{Gn}(ref) = &C_p\Delta x_p^{Gn} + C_i^p\Delta i^{Gn} + C_{Gn}^v\Delta v^{Gn} \\ &+ C_{Sn}^v\Delta v^{Sn} + D_{Gn}^u\Delta u_{Gn}.\end{aligned} \tag{20}$$

B. $d-q$ Current Controller

Decoupled controls of d- and q-components of the converter output currents are achieved by two identical PI controllers shown in Fig. 14. The input to this block is the vector of reference currents $\Delta i^{Gn}(ref)$ determined by the power management block, and the output is the voltage reference vector corresponding to the converter output voltages $\Delta v^{Sn}(ref)$ (see Fig. 7). The state-space representation of the $d-q$ current control block is

$$\Delta \dot{x}_c^{Gn} = A_c\Delta x_c^{Gn} + E_i^c\Delta i^{Gn} + B^i\Delta i^{Gn}(ref) \tag{21}$$

where Δx_c^{Gn} is the state vector composed of state variables for the $d-q$ PI controllers. The output signal from this block is

$$\Delta v^{Sn}(ref) = C_c\Delta x_c^{Gn} + C_i^c\Delta i^{Gn} + C_{Gn}^c\Delta v^{Gn} + D^c\Delta\omega_n. \tag{22}$$

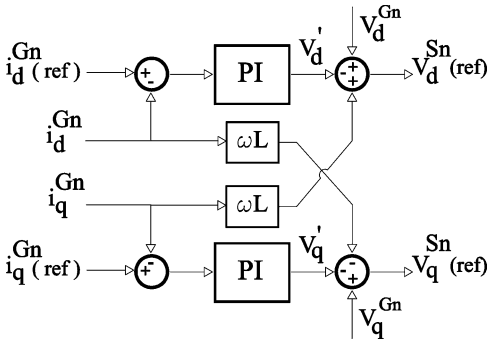

Fig. 14. $d-q$ current controllers for an EI-DG.

A detailed procedure to build (21) and (22) is given in [8].

C. Power Circuit

The power circuit of an EI-DG unit is represented by a three-phase VSC interfaced through coupling impedances to the utility system. The VSC is equipped with a built-in pulse-width modulation (PWM) block, which utilizes the vector of reference voltages determined by the dq-current control block to generate the corresponding gating signals for the converter switches and to synthesize a controlled sinusoidal terminal voltages. The dynamic model of the ac-side power circuit, in the abc frame, is obtained from the ODEs of the three phases as

$$v_{abc}^{Sn} = -R_s i_{abc}^{Gn} - L_s \frac{d}{dt} i_{abc}^{Gn} + v_{abc}^{Gn} \tag{23}$$

where v_{abc}^{Sn}, v_{abc}^{Gn}, and i_{abc}^{Gn} are vectors of instantaneous values of the converter ac-side voltages, bus voltages, and the converter ac-side currents, respectively. The equivalent impedance of the coupling inductances and isolating/step-up transformer are represented by series connected R_s and L_s elements in each phase (see Fig. 2). The state-space model of the power converter is derived from (23), in which the vector of d- and q-components of the converter currents Δx_e^{Gn} represents the state vector, the vector of reference voltages $\Delta v^{Sn}(ref)$, and the vector of monitored bus voltages Δv^{Gn} are input signals (see Fig. 7). The state-space representation is

$$\Delta \dot{x}_e^{Gn} = A_e \Delta x_e^{Gn} + B_{Gn}^e \Delta v^{Gn} + B_{Sn}^e \Delta v_{ref}^{Sn} \tag{24}$$

$$\Delta i^{Gn} = \Delta x_e^{Gn}. \tag{25}$$

The overall small-signal model of an EI-DG unit is constituted from (19), (21), and (24) with the state vector of

$$\Delta x_{Gn} = \begin{bmatrix} \Delta x_e^{Gn} & \Delta x_c^{Gn} & \Delta x_p^{Gn} \end{bmatrix}^T$$

and the input vector of

$$\Delta u_{Gn} = \begin{bmatrix} \Delta P_{Gn}^o & \Delta V^{Gn}(ref) & \Delta v_q^{Gn} & \Delta v_d^{Gn} \end{bmatrix}^T.$$

APPENDIX C
SMALL-SIGNAL MODEL OF A CONVENTIONAL DG UNIT

A similar approach, as discussed in Appendix B, is used to derive a small-signal dynamic model of a conventional DG unit that is interfaced to the microgrid through a rotating machine. Assuming a synchronous generator-based DG unit, the corresponding electromechanical and control systems are categorized as the three internally related blocks of 1) governor and excitation systems that control real and reactive power outputs of the DG unit, 2) mechanical and rotational parts, including the prime-mover, damper windings, and filed winding of the rotor, and 3) electrical circuit of the stator as the interface medium (see Fig. 7). A state-space model for the mth conventional DG unit is

$$\Delta \dot{x}_{Gm} = A_{Gm} \Delta x_{Gm} + B_{Gm}^v \Delta v^{Gm} + B_{Gm}^u \Delta u_{Gm} \tag{26}$$

where Δx_{Gm} is the state vector, Δv_{Gm} is the vector of the bus voltages, and Δu_{Gm} is the vector of inputs for the mth DG unit. The dynamic model of a conventional DG unit is described in [16], and the detailed procedure to construct (26) from the ODEs representing each block is given in [8].

ACKNOWLEDGMENT

The authors would like to thank Prof. P. W. Lehn for his constructive comments and suggestions.

REFERENCES

[1] N. D. Hatziargyriou and A. P. S. Meliopoulos, "Distributed energy sources: Technical challenges," in *Proc. IEEE Power Eng. Soc. Winter Meeting*, New York, Jan. 2002, vol. 2, pp. 1017–1022.

[2] C. L. Smallwood, "Distributed generation in autonomous and non-autonomous micro grids," in *Proc. IEEE Rural Electric Power Conf.*, May 2002, pp. D1/1–D1/6.

[3] R. H. Lasseter and P. Piagi, "Microgrid: A conceptual solution," in *Proc. Power Electronics Specialists Conf.*, Aachen, Germany, Jun. 2004, vol. 6, pp. 4285–4290.

[4] B. Rabelo and W. Hofmann, "Optimal active and reactive power control with the doubly-fed induction generator in the MW-class wind-turbines," in *Proc. 4th IEEE Int. Conf. Power Electronics Drive Systems*, Oct. 2001, pp. 53–58.

[5] J. V. Milanovic and T. M. David, "Stability of distributed networks with embedded generators and induction motors," in *Proc. IEEE Power Eng. Soc. Winter Meeting*, New York, Jan. 2002, vol. 2, pp. 1023–1028.

[6] F. Katiraei, M. R. Iravani, and P. W. Lehn, "Micro-grid autonomous operation during and subsequent to islanding process," *IEEE Trans. Power Del.*, vol. 20, no. 1, pp. 248–257, Jan. 2005.

[7] C. Schauder and H. Mehta, "Vector analysis and control of the advanced static VAr compensators," *Proc. Inst. Elect. Eng., Gen., Transm., Distrib.*, vol. 140, no. 4, pp. 299–306, Jul. 1993.

[8] F. Katiraei, M. R. Iravani, and P. W. Lehn, "Small-signal dynamic model of a micro-grid including conventional and electronically-interfaced distributed resources," *Proc. Inst. Elect. Eng., Gen., Transm., Distrib.*, accepted for publication.

[9] U. Borup, F. Blaabjerg, and P. Enjeti, "Sharing of nonlinear load in parallel-connected three-phase converters," *IEEE Trans. Ind. Appl.*, vol. 37, no. 6, pp. 1817–1823, Nov./Dec. 2001.

[10] M. C. Chandorkar, D. M. Divan, and B. Banerjee, "Control of distributed UPS systems," in *Proc. Power Eng. Conf. Rec.*, Jun. 1994, vol. 1, pp. 197–204.

[11] S. K. Chung, "A phase tracking system for three phase utility interface inverters," *IEEE Trans. Power Electron.*, vol. 15, no. 3, pp. 431–438, May 2000.

[12] E. A. A. Coelho, P. C. Cortizo, and P. F. D. Garcia, "Small-signal stability for parallel-connected inverters in stand-alone AC supply systems," *IEEE Trans. Ind. Appl.*, vol. 38, no. 2, pp. 533–542, Mar./Apr. 2002.

[13] F. Z. Peng, J. W. McKeever, and D. J. Adams, "A power line conditioner using cascaded multilevel inverters for distribution systems," *IEEE Trans. Ind. Appl.*, vol. 34, no. 6, pp. 1293–1298, Nov./Dec. 1998.

[14] F. Katiraei, "Dynamic analysis and control of distributed energy resources in a micro-grid," Ph.D. dissertation, Univ. Toronto, Toronto, ON, Canada, 2005.

[15] P. Kundur, *Power System Stability and Control*. New York: McGraw-Hill, 1994.

[16] P. C. Krause, *Analysis of Electric Machinery and Drive Systems*. Piscataway, NJ: IEEE Press, 2002.

F. Katiraei (S'01–M'05) received the B.Sc. and M.Sc. degrees in electrical engineering from Isfahan University of Technology, Isfahan, Iran, in 1995 and 1998, respectively, and the Ph.D. degree in electrical engineering from the University of Toronto, Toronto, ON, Canada, in 2005.

He is currently a T&D Research Engineer at the CANMET Energy Technology Center, Varennes, QC, Canada. His interested research areas include power electronic applications on power systems and distributed energy generation systems for microgrid applications and development.

M. R. Iravani (M'85–SM'00–F'03) received his B.Sc. degree in electrical engineering in 1976 from Tehran Polytechnique University, Tehran, Iran, and the M.Sc. and Ph.D. degrees in electrical engineering from the University of Manitoba, Winnipeg, MB, Canada in 1981 and 1985, respectively.

He started his career as a Consulting Engineer. Presently, he is a Professor at the University of Toronto, Toronto, ON, Canada. His research interests include power electronics and power system dynamics and control.